Mon. Not. R. Astron. Soc. **377,** 1481–1487 (2007) doi:10.1111/j.1365-2966.2007.11682.x

Destabilization of hydrodynamically stable rotation laws by azimuthal magnetic fields

Günther Rüdiger,[1]★ Rainer Hollerbach,[2] Manfred Schultz[1] and Detlef Elstner[1]

[1]*Astrophysikalisches Institut Potsdam, An der Sternwarte 16, D-14482 Potsdam, Germany*
[2]*Department of Applied Mathematics, University of Leeds, Leeds LS2 9JT*

Accepted 2007 February 28. Received 2007 February 27; in original form 2007 January 12

ABSTRACT

We consider the effect of toroidal magnetic fields on hydrodynamically stable Taylor–Couette differential rotation flows. For current-free magnetic fields a non-axisymmetric $m = 1$ magnetorotational instability arises when the magnetic Reynolds number exceeds $O(100)$. We then consider how this 'azimuthal magnetorotational instability' (AMRI) is modified if the magnetic field is not current-free, but also has an associated electric current throughout the fluid. This gives rise to current-driven Tayler instabilities (TIs) that exist even without any differential rotation at all. The interaction of the AMRI and the TI is then considered when both electric currents and differential rotation are present simultaneously. The magnetic Prandtl number *Pm* turns out to be crucial in this case. Large *Pm* have a destabilizing influence, and lead to a smooth transition between the AMRI and the TI. In contrast, small *Pm* have a stabilizing influence, with a broad stable zone separating the AMRI and the TI. In this region the differential rotation is acting to stabilize the TIs, with possible astrophysical applications (Ap stars). The growth rates of both the AMRI and the TI are largely independent of *Pm*, with the TI acting on the time-scale of a single rotation period, and the AMRI slightly slower, but still on the basic rotational time-scale. The azimuthal drift time-scale is ∼20 rotations, and may thus be a (flip-flop) time-scale of stellar activity between the rotation period and the diffusion time.

Key words: MHD – Sun: rotation – stars: magnetic fields.

1 INTRODUCTION

We consider the problem of how linear hydrodynamic and magnetohydrodynamic instabilities interact in a simple rotating shear flow, the familiar Taylor–Couette flow between concentric cylinders. In the purely hydrodynamic problem, the Rayleigh criterion states that an ideal flow is stable against axisymmetric perturbations when the specific angular momentum increases outwards

$$\frac{\mathrm{d}}{\mathrm{d}R}(R^2\Omega)^2 > 0, \tag{1}$$

where Ω is the angular velocity, and cylindrical coordinates (R, ϕ, z) are used. Viscosity has a stabilizing effect, so that a Taylor–Couette flow that violates (1) becomes unstable only if the angular velocity of the inner cylinder (i.e. its Reynolds number) exceeds some critical value.

If a uniform axial magnetic field is included, a new type of instability arises, the magnetorotational instability (MRI). The Rayleigh criterion is then replaced by

$$\frac{\mathrm{d}}{\mathrm{d}R}\Omega^2 > 0. \tag{2}$$

That is, the requirement for stability is that the angular velocity itself increases outward, rather than the angular momentum. This is more stringent than (1), so a flow may be hydrodynamically stable, but magnetohydrodynamically unstable. And again, viscosity and/or magnetic diffusivity have a stabilizing effect; for small magnetic Prandtl numbers it is the magnetic Reynolds number that must exceed a critical value for instability to occur (Rüdiger, Schultz & Shalybkov 2003). Hollerbach & Rüdiger (2005) considered how the MRI is modified if an azimuthal field $B_\phi \propto R^{-1}$ is added, and found that the relevant parameter is then the ordinary Reynolds number *Re*, rather than the magnetic Reynolds number *Rm*.

In this work we will consider instabilities of purely azimuthal magnetic fields, without any axial field being present. We begin by showing that even $B_\phi \propto R^{-1}$ by itself supports an MRI. This new type of MRI is non-axisymmetric, having azimuthal wavenumber $m = 1$, but otherwise shares all the characteristics of the classical, axisymmetric MRI in an axial field. These results are presented in Section 3.

We then extend the choice of imposed field to be of the form $B_\phi = a_B R + b_B R^{-1}$. The part $b_B R^{-1}$ corresponds to an axial current only within the inner cylinder $R < R_{\rm in}$, so current-free within the fluid, but the part $a_B R$ corresponds to a uniform axial current density $J_z =$

★E-mail: gruediger@aip.de

$2a_B$ everywhere within $R < R_{\rm out}$. Taking $B_\phi = a_B R + b_B R^{-1}$ instead of just $B_\phi = b_B R^{-1}$ has profound implications, well beyond simply having a somewhat different radial profile. In particular, if there are no electric currents flowing within the fluid ($a_B = 0$), the only source of energy to drive instabilities is the differential rotation; the magnetic field merely acts as a catalyst, not as a source of energy. For $Re = 0$ no instabilities are thus possible, regardless of how strong the magnetic field is.

In contrast, if there are electric currents flowing within the fluid ($a_B \neq 0$), this yields a new source of energy to drive purely magnetic instabilities, that may exist even at $Re = 0$. Michael (1954), Velikhov (1959) and Vandakurov (1972) considered axisymmetric magnetic instabilities and derived the stability criterion

$$\frac{\rm d}{{\rm d}R}\left(\frac{B_\phi}{R}\right)^2 < 0. \tag{3}$$

Vandakurov (1972) and Tayler (1973) also included non-axisymmetric disturbances. It was shown that for an ideal fluid the necessary and sufficient condition for stability is

$$\frac{\rm d}{{\rm d}R}\left(RB_\phi^2\right) < 0 \tag{4}$$

(Tayler 1973). A *uniform* field would therefore be axisymmetrically stable, but non-axisymmetrically unstable, with $m = 1$ being the most unstable mode. The profile $B_\phi \propto R^{-1}$ is stable according to both (3) and (4), in agreement with the discussion above, that for such a current-free profile there is simply no source of energy to drive purely magnetic instabilities.

In Section 4 we then choose a_B and b_B such that B_ϕ is as uniform as possible, with the same values at $R_{\rm in}$ and $R_{\rm out}$. We consider how the resulting Tayler instabilities (TIs) interact with the azimuthal magnetorotational instability (AMRI) presented in Section 3. We find that the magnetic Prandtl number plays a key role: if $Pm \gtrsim 10$ the AMRI and the TI are smoothly connected to one another, but if $Pm \lesssim 1$ they are disconnected, with a region of stability separating them.

The results presented here have important astrophysical implications, since the simultaneous existence of differential rotation and toroidal magnetic fields is characteristic of almost all celestial bodies. Prominent examples of differentially rotating objects with large magnetic Prandtl number are protogalaxies (without supernova explosions) and protoneutron stars (PNS). Even rather weak toroidal fields should be unstable in these objects. In contrast, the radiative zones of stars have $Pm < 10^{-2}$. In this case we will see that the toroidal field is *stabilized*, as long as it is not too strong. Finally, in the limit of no differential rotation, the pure TI is independent of Pm.

2 BASIC EQUATIONS

We consider a viscous, electrically conducting, incompressible fluid between two rotating infinite cylinders, in the presence of an azimuthal magnetic field. The equations of the problem are

$$\frac{\partial \boldsymbol{U}}{\partial t} + (\boldsymbol{U}\cdot\nabla)\boldsymbol{U} = -\frac{1}{\rho}\nabla P + \nu\Delta\boldsymbol{U} + \frac{1}{\mu_0\rho}{\rm rot}\boldsymbol{B}\times\boldsymbol{B},$$
$$\frac{\partial \boldsymbol{B}}{\partial t} = {\rm rot}\,(\boldsymbol{U}\times\boldsymbol{B}) + \eta\Delta\boldsymbol{B} \tag{5}$$

and

$${\rm div}\,\boldsymbol{U} = {\rm div}\,\boldsymbol{B} = 0, \tag{6}$$

where $\boldsymbol{U}$ is the velocity, $\boldsymbol{B}$ the magnetic field, P the pressure, ν the kinematic viscosity, and η the magnetic diffusivity. Equations (5) yield the basic state solution:

$$U_R = U_z = B_R = B_z = 0 \tag{7}$$

and

$$U_\phi = R\Omega = a_\Omega R + \frac{b_\Omega}{R}, \qquad B_\phi = a_B R + \frac{b_B}{R}. \tag{8}$$

a_Ω and b_Ω are given by

$$a_\Omega = \Omega_{\rm in}\frac{\hat\mu_\Omega - \hat\eta^2}{1-\hat\eta^2}, \qquad b_\Omega = \Omega_{\rm in}R_{\rm in}^2\frac{1-\hat\mu_\Omega}{1-\hat\eta^2}, \tag{9}$$

where

$$\hat\eta = \frac{R_{\rm in}}{R_{\rm out}}, \qquad \hat\mu_\Omega = \frac{\Omega_{\rm out}}{\Omega_{\rm in}}. \tag{10}$$

$\Omega_{\rm in}$ and $\Omega_{\rm out}$ are the imposed rotation rates of the inner and outer cylinders, with radii $R_{\rm in}$ and $R_{\rm out}$.

In contrast to U_ϕ, where a_Ω and b_Ω are merely derived quantities ($\Omega_{\rm in}$ and $\Omega_{\rm out}$ being the fundamental quantities), for B_ϕ, a_B and b_B themselves are the fundamental quantities; as previously noted, $a_B R$ corresponds to a uniform axial current everywhere within $R < R_{\rm out}$, and $b_B R^{-1}$ corresponds to an additional current only within $R < R_{\rm in}$. In analogy with $\hat\mu_\Omega$, it is useful though to define the quantity

$$\hat\mu_B = \frac{B_{\rm out}}{B_{\rm in}} = \frac{a_B R_{\rm out} + b_B R_{\rm out}^{-1}}{a_B R_{\rm in} + b_B R_{\rm in}^{-1}}, \tag{11}$$

measuring the variation in B_ϕ across the gap.

In Section 3 we consider the field $B_\phi \propto R^{-1}$, so $a_B = 0$ and $b_B = 1$. In contrast, in Section 4 we include non-zero a_B, and adjust it so that $\hat\mu_B = 1$, so the toroidal field profile is as uniform as possible (see also Cally 2003). Taking $R_{\rm in} = 1$ and $R_{\rm out} = 2$, this corresponds to setting $a_B = 1/3$ and $b_B = 2/3$; B_ϕ then varies by less than 6 per cent across the gap.

We are interested in the linear stability of the solution (8). The perturbed state of the flow is described by

$$u_R,\ R\Omega + u_\phi,\ u_z,\ b_R,\ B_\phi + b_\phi,\ b_z. \tag{12}$$

Developing the disturbances into normal modes, solutions of the linearized equations are considered in the form

$$F = F(R)\exp\left[{\rm i}(kz + m\phi + \omega t)\right], \tag{13}$$

where F is any of the perturbation quantities.

The magnetic Prandtl number (Pm), the Hartmann number (Ha) and the Reynolds number (Re) are the dimensionless numbers of the problem,

$$Pm = \frac{\nu}{\eta}, \qquad Ha = \frac{B_{\rm in}R_0}{\sqrt{\mu_0\rho\nu\eta}}, \qquad Re = \frac{\Omega_{\rm in}R_0^2}{\nu}, \tag{14}$$

where $R_0 = [R_{\rm in}(R_{\rm out} - R_{\rm in})]^{1/2}$ is taken as the unit of length. We have used R_0^{-1} as the unit of the wave number, η/R_0 as the unit of the velocity fluctuations, $\Omega_{\rm in}$ as the unit of frequencies, and $B_{\rm in}$ as the unit of the magnetic field fluctuations. Where appropriate, we will also use the magnetic Reynolds number

$$Rm = Pm\cdot Re \tag{15}$$

and the Lundquist number

$$S = \sqrt{Pm}\cdot Ha. \tag{16}$$

A set of 10 boundary conditions is needed to solve the equations, namely, no-slip

$$u_R = u_\phi = u_z = 0 \tag{17}$$

for the flow, and perfectly conducting

$$\frac{\mathrm{d}b_\phi}{\mathrm{d}R} + \frac{b_\phi}{R} = b_R = 0 \tag{18}$$

for the field, both sets being applied at both $R_{\rm in}$ and $R_{\rm out}$. If the exterior regions were taken to be insulators, the boundary conditions on the field would be different (e.g. Rüdiger et al. 2003; Shalybkov 2006), but here we will consider only conducting boundary conditions.

The system of linearized equations and associated boundary conditions then constitutes a one-dimensional linear eigenvalue problem, solved by finite-differencing in radius as in Rüdiger et al. (2005). Typically, around 100 grid points were used, and all results were checked to ensure that they were fully resolved.

3 THE AZIMUTHAL MAGNETOROTATIONAL INSTABILITY

The rotation laws in stars and galaxies are hydrodynamically stable. Such rotation laws can be modelled by Taylor–Couette containers with rotating outer cylinder. More precisely, the rotation of the outer cylinder must fulfil the Rayleigh condition, $\hat{\mu} > \hat{\eta}^2$. The containers considered here have $\hat{\eta} = 0.5$, so that a flow with $\hat{\mu} = 0.5$ is clearly beyond the Rayleigh limit where the hydrodynamic instability disappears. Such a rotation law, however, can become unstable against non-axisymmetric disturbances under the presence of a current-free toroidal field. Fig. 1 shows stability curves for $m = 1$, the only mode that appears to become unstable. We see how an MRI exists that is remarkably similar to the classical MRI with a purely axial field. In particular, as $Pm \to 0$, the relevant parameters are also Rm and S, with the MRI arising if $Rm \gtrsim 80$, and $S \approx 40$ yielding the lowest value of $\mathrm{Rm_c}$. The specific numbers are roughly an order of magnitude greater than for the axisymmetric MRI in the axial field (cf. Rüdiger et al. 2003), but the basic scalings, and even the detailed shape of the instability curves, are identical.

Fig. 2 shows the real and imaginary parts of $\mathrm{i}\omega$ in the unstable regime. Remembering that time has been scaled by $\Omega_{\rm in}^{-1}$, we see that we obtain growth rates as large as $0.05\Omega_{\rm in}$. So again, while the particular number 0.05 is about an order of magnitude smaller than for the axisymmetric MRI in the axial field, this non-axisymmetric MRI is clearly also growing on the basic rotational time-scale.

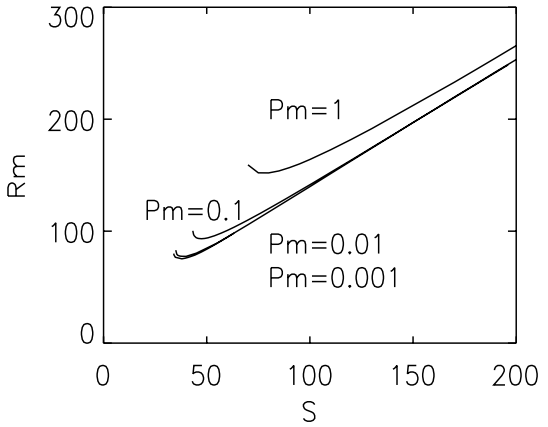

Figure 1. The marginal stability domains for the $m = 1$ AMRI with $\hat{\eta} = 0.5$ conducting cylinders. The outer cylinder rotates with 50 per cent of the rotation rate of the inner one, $\hat{\mu}_\Omega = 0.5$; the magnetic field between the cylinders is current-free, $\hat{\mu}_B = 0.5$. The curves are marked with their magnetic Prandtl numbers.

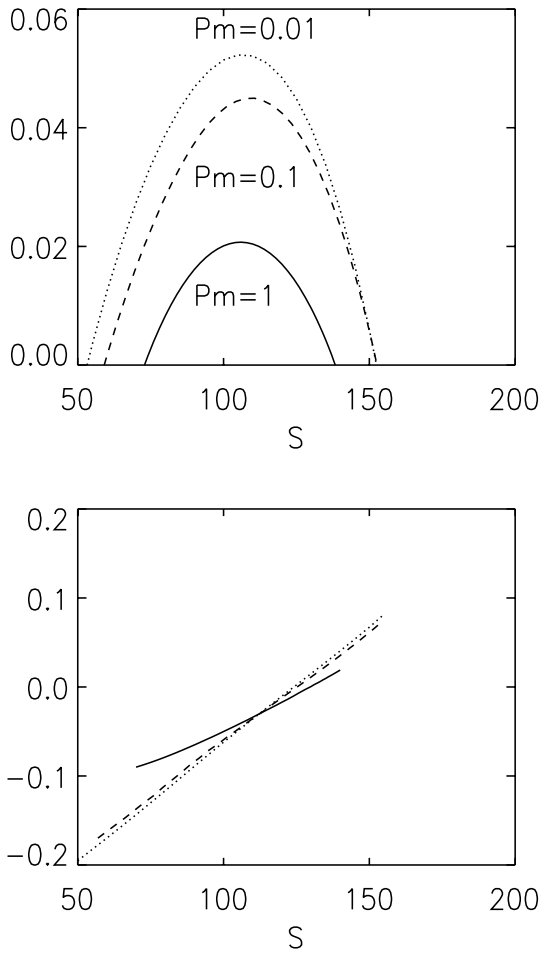

Figure 2. The growth rates (top) and azimuthal drift rates (bottom), as functions of S, with Rm fixed at 200.

To understand why this non-axisymmetric MRI exists even for a purely toroidal field $\boldsymbol{B}_0$, for which it is known that the axisymmetric MRI fails, we need to consider the R and ϕ components of the induction equation

$$\begin{aligned} Rm\,\mathrm{i}\omega b_R = {} & \Delta b_R - R^{-2} b_R - 2\mathrm{i}m R^{-2} b_\phi \\ & + \mathrm{i}m R^{-2} u_R - Rm\,\mathrm{i}m\Omega\, b_R, \end{aligned} \tag{19}$$

$$\begin{aligned} Rm\,\mathrm{i}\omega b_\phi = {} & \Delta b_\phi - R^{-2} b_\phi + 2\mathrm{i}m R^{-2} b_R \\ & + \mathrm{i}m R^{-2} u_\phi + 2R^{-2} u_R - Rm\,\mathrm{i}m\Omega\, b_\phi + Rm\, R \frac{\mathrm{d}\Omega}{\mathrm{d}R} b_R. \end{aligned} \tag{20}$$

In particular, note that for $m = 0, b_R$ completely decouples from everything else, and inevitably decays away. Without b_R though, the MRI cannot proceed, as it relies on the term $R(\mathrm{d}\Omega/\mathrm{d}R)b_R$. In contrast, for $m = 1, b_R$ is coupled both to b_ϕ, coming from $\Delta\boldsymbol{b}$, and to u_R, from rot $(\boldsymbol{u} \times \boldsymbol{B}_0)$. And once b_R is coupled to the rest of the problem, the term $R(\mathrm{d}\Omega/\mathrm{d}R)b_R$ then allows the MRI to develop. A detailed examination of the structure of the solutions shows that all three components of both $\boldsymbol{u}$ and $\boldsymbol{b}$ are indeed present.

We emphasize also that this indeed is an MRI, and not a pinch, Tayler or other current-driven instability. Once again, for a current-free field all current-driven instabilities are excluded a priori. What we have here is that a magnetic field, which by itself would be stable at any amplitude, acts as a catalyst and destabilizes a

hydrodynamically stable differential rotation, just as in the classical MRI. We note though that there is no hope of realizing this AMRI in the laboratory; not only is the critical magnetic Reynolds number rather large, but beyond that, achieving a sufficiently strong toroidal field would require enormously large electric currents, beyond what could reasonably be imposed.

4 THE TAYLER INSTABILITY

Having demonstrated that the current-free field $B_\phi = R^{-1}$ yields this non-axisymmetric AMRI, we next wish to consider what effect including currents within the fluid ($a_B \neq 0$) has. There are two questions one might wish to address here. First, how robust is the AMRI in this case; does it continue to exist at all, and if so, are the growth and drift rates much the same? Secondly, as discussed in the introduction, if there are currents flowing within the fluid, then for sufficiently great Hartmann numbers TIs exist (here $Ha_{\rm Tayler} \simeq 150$), which also turn out to be $m = 1$, and could thus be expected to interact in some significant way with the AMRI. In this section we therefore consider the nature of this interaction between the AMRI and the TI, and in particular how it depends on the magnetic Prandtl number Pm.

Generally, as one can read from Fig. 3 fast rotation is stabilizing and strong toroidal fields are stabilizing (Pitts & Tayler 1985). However, large magnetic Prandtl numbers also prove to be strongly destabilizing (Fig. 3, top). The right-half of the AMRI branch, the one for strong magnetic fields, disappears completely. Instead, the critical Rm decreases monotonically with Ha until eventually $Ha_{\rm Tayler} \simeq 150$ is reached. The transition from the AMRI to the TI is smooth, without any striking features.

However, for $Pm \lesssim 1$ the stable right-hand branch of the AMRI in Fig. 1 reappears. There is always a domain between the AMRI and the TI where the flow is *stable*, despite the large magnetic fields, $Ha > Ha_{\rm Tayler}$), that is, in a regime where the field without a differential rotation would be unstable. Roughly speaking, according to the results in Fig. 3 (bottom), the TI exists for sufficiently strong magnetic field, that is,

$$S \gg Rm \tag{21}$$

and the AMRI exists for sufficiently weak magnetic field, that is,

$$S \ll Rm \tag{22}$$

(for $Pm \lesssim 1$). With the magnetic velocity $v_{\rm A} = B_\phi/\sqrt{\mu_0 \rho}$ and the linear rotation speed $U_\phi = R_{\rm in}\,\Omega_{\rm in}$ then

$$\frac{v_{\rm A}}{U_\phi} \gg \frac{\Delta R}{R} \tag{23}$$

for TI and

$$\frac{v_{\rm A}}{U_\phi} \ll \frac{\Delta R}{R} \tag{24}$$

for AMRI. Here $\Delta\, R/R$ is the fractional layer thickness which is of the order of unity in our model while for the solar tachocline its value is about 0.05. The AMRI and TI are separated by an extended stable domain where $v_{\rm A}/U_\phi \approx \Delta\, R/R$.

For small Pm and for sufficiently high Reynolds number a second (smaller) critical Hartmann number exists so that depending on the initial conditions two different stable solutions are possible. A solution with growing amplitude (e.g. dynamo-induced) becomes unstable already at $Ha \simeq 50$ while a decaying magnetic field (e.g. after collapse) already becomes stable at $Ha > 150$.

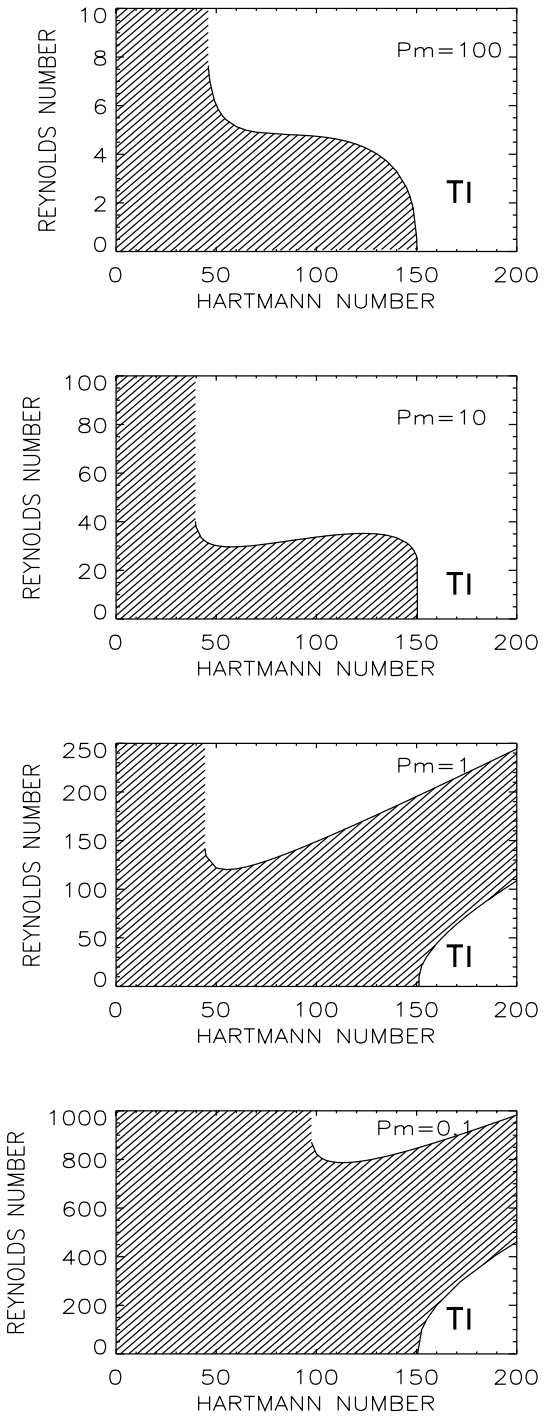

Figure 3. The marginal stability domains (hatched) for the $m = 1$ TI and AMRI together, for $\hat{\eta} = 0.5$ conducting cylinders. The outer cylinder rotates with 50 per cent of the rotation rate of the inner one, $\hat{\mu}_\Omega = 0.5$; the magnetic field between the cylinders is as uniform as possible, $\hat{\mu}_B = 1$. The panels are marked with their magnetic Prandtl numbers.

For our special magnetic field profile ($\hat{\mu}_B = 1$) and for sufficiently large Reynolds numbers, the lower critical Hartmann number moves from 150 for small Pm to about 50 for large Pm (see Fig. 3). Large Pm are destabilizing, and small Pm are stabilizing (Kurzweg 1963). However, even for $Pm > 100$, we did not find smaller values than $Ha \simeq 50$. This finding is important for objects with very high magnetic Prandtl number like PNS and protogalaxies. They can

possess stable toroidal magnetic fields of finite value, up to $Ha \simeq 50$.

Obviously, for very small magnetic Prandtl number the AMRI becomes less and less important. Magnetic fields with $Ha < Ha_{\rm Tayler}$ are stable for almost all Re. For $Ha > Ha_{\rm Tayler}$ this zone of stability separating the AMRI and TI branches plays an important role though. For a broad range of Reynolds numbers even strong magnetic fields are stabilized against the TI.

5 GROWTH RATES

As we have demonstrated with Fig. 2 (top) the current-free AMRI shown in Fig. 1 has growth rates $\gamma = -\Im(\omega)$ of around $0.05\Omega_{\rm in}$, only very weakly dependent on Pm. To characterize the instabilities with weak currents we compute the complex frequency and the wave number in the instability domain shown in Fig. 3 for two values of Pm and for two particular, sufficiently large Reynolds numbers. On both the limiting magnetic fields, of course, the growth rate vanishes. Its maximal value between both the limits is (here) 0.004 (see Fig. 4). That there is a proportionality $\gamma \propto Ha^2$ of the growth rate as suggested by Spruit (1999, his equation 37) cannot be confirmed.

The resulting growth rate of only 0.004 means that the instability grows with a characteristic time of about 40 rotation periods of the inner cylinder, that is, for 20 rotation periods of the outer cylinder. It is a rather slow instability. However, the growth rates also depend on the Reynolds number. They are very small close to the marginal stability limit and they grow with growing Reynolds number. For slightly supercritical Reynolds numbers one finds for $Pm = 1$ the growth rate expression $\gamma \simeq (Re - Re_{\rm crit})/1333$ with $Re_{\rm crit} = 119$ (Fig. 5, left-hand panel). The faster the rotation the faster the growth rate, but there is a saturation of the growth rates, which does not depend strongly on Pm (see Fig. 5, right-hand panel). The saturation value for $Pm = 1$ is about 0.12 and for (the more realistic) $Pm = 0.1$ it is about 0.10. This maximum growth rate translates into about 1.5 rotation times of the inner cylinder. Note therefore that the AMRI is a fast instability for turbulent media with their typical value of $Pm \leqslant 1$, but it may be slower for the laminar gas of radiative stellar cores ($Pm \leqslant 10^{-2}$ to 10^{-3}).

The main sequence stars of spectral class A as a group are fast rotators with high Reynolds numbers. The magnetic Ap stars are the slower rotators in the group so that they should have smaller Reynolds numbers than the non-magnetic A stars. Inspecting Fig. 3 (for small magnetic Prandtl number, bottom) one may speculate that the A stars as a group are located at the limit between AMRI and the stability branch. Then the Ap stars would lie in the slow-rotation stable regime while the non-magnetic A stars would lie in the unstable AMRI regime. Toroidal fields induced by differential rotation of the order of 10^7 G would then be stable for the slow rotators (Ap) and unstable for the fast rotators (A). It is necessary, however, for this kind of theory of the Ap stars that in Fig. 3 (bottom) the differential-rotation-induced stable domain also exists for sufficiently high Reynolds numbers and Hartmann numbers, which is still unknown (cf. Braithwaite & Spruit 2004).

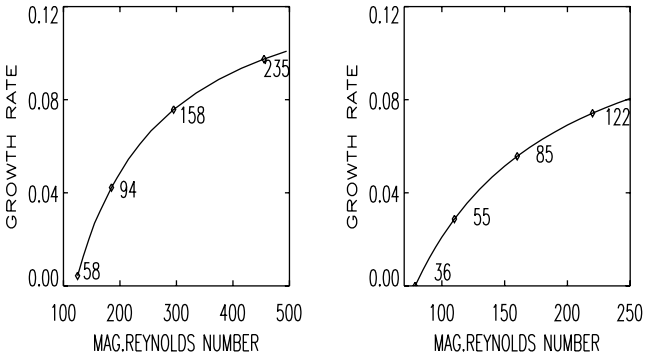

Figure 5. The growth rate shown in Fig. 4 for growing magnetic Reynolds numbers Rm for $Pm = 1$ (left-hand panel) and $Pm = 0.1$ (right-hand panel). The curves are marked with the Lundquist numbers S for which the growth rates have a maximum.

The TI seems to be faster than the AMRI. The growth rates show that only (say) one rotation time is enough to develop the instability. The growth rate presented in Fig. 6 scales linearly with the magnetic field. This result clearly confirms the early finding of Goossens, Bironi & Tayler (1981) who found for non-rotating stars with toroidal fields the relation

$$\gamma \gtrsim \frac{B_\phi}{\sqrt{\mu_0 \rho} R} \tag{25}$$

for the growth rate. Translated to our notation this might mean

$$\frac{\gamma}{\Omega} \gtrsim \frac{Ha}{Re\sqrt{Pm}}, \tag{26}$$

leading to values exceeding unity in accordance to their numerical results (their table 1). For a typical A star Goossens & Veugelen (1978) find 50–500 d. The values in Fig. 6 which we obtained under the presence of rotation are of the same order, leading to growth times of one rotation period.

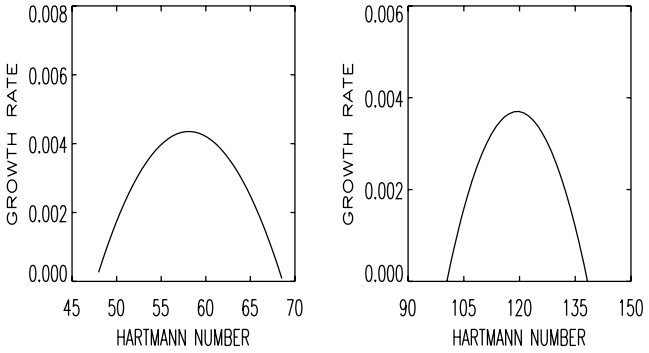

Figure 4. The growth rate for the AMRI with weak currents (see Fig. 3) for $Pm = 1$ (left-hand panel, here $Rm = 125$) and for $Pm = 0.1$ (right-hand panel, here $Rm = 82$).

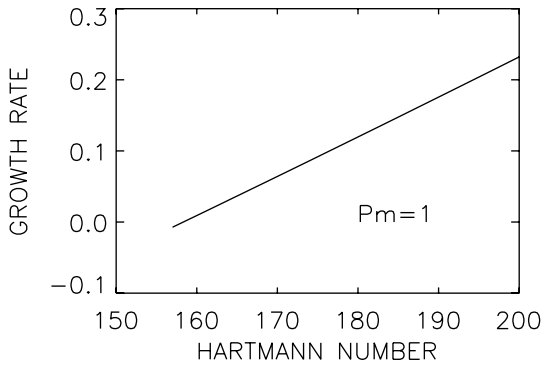

Figure 6. The growth rates for $Pm = 40$ in the TI corner of Fig. 3 (middle, $Pm = 1$). Note that the growth rates for TI are higher than for AMRI and that they vary linearly with the magnetic field.

Note that equation (26) can be rewritten as

$$\frac{\gamma}{\Omega} \gtrsim \frac{B_{\rm in}}{\sqrt{\mu_0\rho}R_0\Omega}, \tag{27}$$

which for the solar interior yields

$$\frac{\gamma}{\Omega} \simeq \frac{B_{\rm in}}{10^6\ {\rm G}}. \tag{28}$$

An internal toroidal field of 1 MG would thus decay in 4 d. The decay time of stronger magnetic fields, such as proposed by Dicke (1979, 100 MG) or Couvidat, Turck-Chièze & Kosovichev (2003, 30 MG), would even be in the order of a few hours (see Goossens & Tayler 1980).

6 AZIMUTHAL DRIFT

For almost all non-axisymmetric phenomena there is an azimuthal drift of the pattern $\dot{\phi} = -\Re(\omega)/m$. Negative (positive) real parts of the frequency ω, therefore, means eastward (westward) migration. If the pattern is considered in the system corotating with the outer cylinder the value 0.5 must be added to the real part of the frequency, which has already been done in Figs 7 and 8. Then the resulting normalized drift is -0.05 in units of the outer rotation, or -0.025 in units of the inner rotation. The negative sign means that the non-axisymmetric pattern rotates *faster* than the outer cylinder. For different Reynolds numbers we found very similar drift rates. For increasing Hartmann numbers, however, the effective drift rate is reduced and eventually changes its sign, but the maximal amplitude remains of the order of 0.05.

The characteristic time for one complete revolution of the pattern is then about 20 rotation times of the outer cylinder, or 1.35 yr if we apply these ideas to the Sun. This time is well-known from various sorts of solar observations (Howe, Komm & Hill 2002; Krivova & Solanki 2002; Ternullo 2007). It is also true that sunspots rotate faster than the solar plasma by about 5 per cent, in agreement with the characteristic time-scale of 20 rotation periods. The time-scale of 20 rotation periods seems to form the long-searched time-scale governing the cycle time of the activity, intermediate between the basic time-scale of one rotation period and the diffusion time-scale.

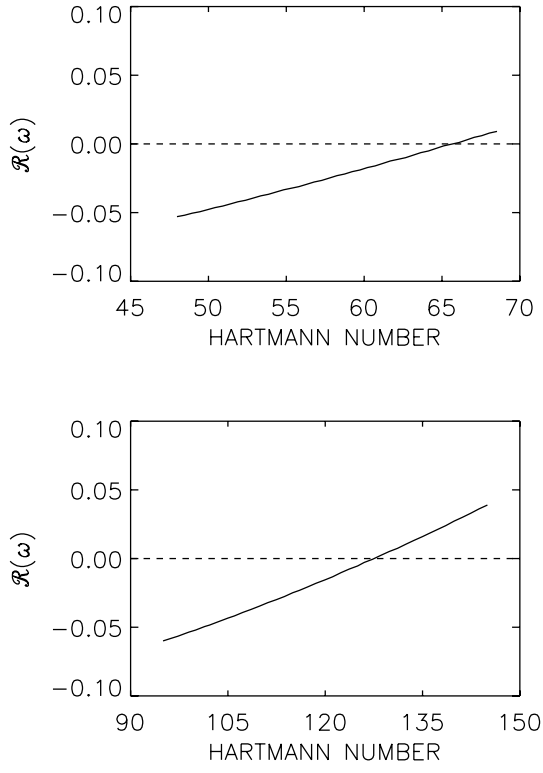

Figure 7. The azimuthal drift for $Pm = 1$ (top, $Rm = 125$) and $Pm = 0.1$ (bottom, $Rm = 82$) hardly depends on the magnetic Prandtl number. $\hat{\mu}_\Omega = 0.5$.

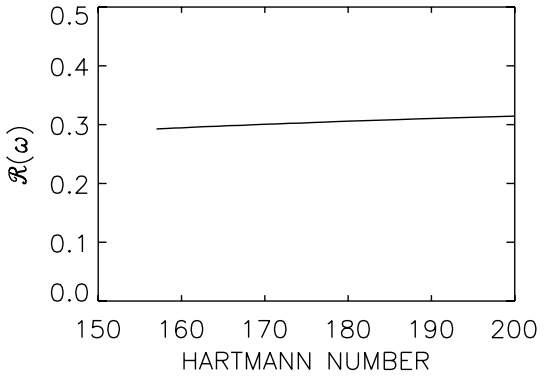

Figure 8. The same as in Fig. 6 but for the drift rate.

The azimuthal drift velocity of the $m = 1$ pattern of the TI appears to be much faster. The value 0.3 given in Fig. 8 does not depend on the field amplitude. It means 4.0 rotation times of the inner cylinder or two rotation times of the outer cylinder. This is a strong effect which cannot be missed by the astrophysical observations. If the flip-flop phenomenon of the FK Coma stars is a result of the TI then the rotation rate of the magnetic pattern should strongly differ from that of the non-magnetic stellar plasma.

7 DISCUSSION

With a simple global model we have demonstrated how the interaction of differential rotation and a toroidal magnetic field works. Our main concern is the presentation of the large influence of the magnetic Prandtl number. The rotation law considered is stable in the hydrodynamic regime. We generally found that a large magnetic Prandtl number is destabilizing, while a small magnetic Prandtl number has a stabilizing influence, and even leads to a broad stable domain between the AMRI and the TI.

Indeed, for large *Pm* the instabilities dominate and stable fields can only exist for very low Reynolds numbers (Fig. 3, top). Almost always toroidal fields with $Ha \simeq 50$ are unstable. For non-turbulent PNS one finds critical magnetic fields of only 1 G and for non-turbulent protogalaxies one finds critical values of only 10^{-18} G. There is no possibility of the existence of stronger toroidal magnetic fields in non-turbulent PNS and non-turbulent protogalaxies.

The opposite is true if turbulent values of the diffusivities are taken into account. Then the effective magnetic Prandtl number in cosmical turbulent fields should be between 0.1 and 1 (Yousef, Brandenburg & Rüdiger 2003). In Table 1 the numerical values are given for the solar convection zone (SCZ) and for a typical galaxy. Note that the Reynolds number for the galaxy basically exceeds the solar value. For galaxies, therefore, the AMRI should occur for Hartmann numbers of the order of 50 (see Fig. 3). A value of about 200 is derived from the galactic parameters used in Table 1 for a magnetic field of (say) 5 μG, which represents the observed magnetic fields. Galaxies are thus suspected to exist nearby or within the AMRI for non-axisymmetric disturbances. The distinct

Table 1. Characteristic values for the SCZ and for a turbulent galaxy.

	ρ (g cm^{-3})	ν (cm^2 s^{-1})	η (cm^2 s^{-1})	B (G)	Ω (s^{-1})	R_0 (cm)	*Re*	*Rm*	*Ha*	*S*
SCZ, top	10^{-3}	10^{13}	10^{12}	10^3	2×10^{-6}	5×10^9	5	50	20	50
SCZ, bottom	10^{-1}	10^{13}	10^{13}	10^4	2×10^{-6}	10^{10}	20	20	10	10
Galaxy	10^{-24}	10^{26}	10^{26}	5×10^{-6}	10^{-15}	10^{22}	1000	1000	200	200

non-axisymmetric ($m = 1$) magnetic geometry of M81 might easily be the result of the existence of the presented non-axisymmetric instabilities of azimuthal fields.

For the turbulent SCZ the Reynolds numbers are so small that for $Pm \leqslant 1$ only the TI limits the magnetic fields. The related Hartmann numbers are about 150. This limit is reached for B_ϕ of the order of 1 kG if the dynamo operates in the supergranulation layer (Brandenburg 2005) or for 100 kG if it is located in the bulk of the SCZ.

This number is even reduced to only 3 kG if – as it is necessary for the operation of advection-dominated solar dynamos – the magnetic diffusivity at the bottom of the convection zone was only 10^{10} cm^2 s^{-1}. In this case all azimuthal fields stronger than 3 kG become unstable against the non-axisymmetric TI and cannot be amplified any more. Generally, for too small magnetic diffusivities (Dikpati & Gilman 2006, are using values between 3×10^{10} and 2×10^{11} cm^2 s^{-1}) the Hartman numbers easily grow beyond the critical value and the non-axisymmetric instabilities – which do not appear in axisymmetric codes – basically limit the magnetic field amplitudes.

REFERENCES

Braithwaite J., Spruit H. C., 2004, Nat, 431, 819
Brandenburg A., 2005, ApJ, 625, 539
Cally P. S., 2003, MNRAS, 339, 957
Couvidat S., Turck-Chièze S., Kosovichev A. G., 2003, ApJ, 599, 1434
Dicke R. H., 1979, ApJ, 228, 898
Dikpati M., Gilman P. A., 2006, ApJ, 649, 498
Goossens M., Veugelen P., 1978, A&A, 70, 277
Goossens M., Tayler R. J., 1980, MNRAS, 193, 833
Goossens M., Biront D., Tayler R. J., 1981, Ap&SS, 75, 521
Hollerbach R., Rüdiger G., 2005, Phys. Rev. Lett., 95, 124501
Howe R., Komm R. W., Hill F., 2002, ApJ, 580, 1172
Krivova N. A., Solanki S. K., 2002, A&A, 394, 701
Kurzweg U., 1963, J. Fluid Mech., 17, 52
Michael D., 1954, Mathematika, 1, 45
Pitts E., Tayler R. J., 1985, MNRAS, 216, 139
Rüdiger G., Schultz M., Shalybkov D., 2003, Phys. Rev. E, 67, 046312
Rüdiger G., Hollerbach R., Schultz M., Shalybkov D., 2005, Astron. Nachr., 326, 409
Shalybkov D., 2006, Phys. Rev. E, 73, 016302
Spruit H. C., 1999, A&A, 349, 189
Tayler R. J., 1973, MNRAS, 161, 365
Ternullo M., 2007, Sol. Phys., 240, 153
Vandakurov Yu. V., 1972, SvA, 16, 265
Velikhov E. P., 1959, SJETP, 9, 995
Yousef T., Brandenburg A., Rüdiger G., 2003, A&A, 411, 321

This paper has been typeset from a TEX/LATEX file prepared by the author.